JOURNAL OF PHYSICAL ORGANIC CHEMISTRY
J. Phys. Org. Chem. 2005; **18:** 901–907
Published online 21 February 2005 in Wiley InterScience (www.interscience.wiley.com). DOI: 10.1002/poc.914

Catalysis of aminolysis of *p*-nitrophenyl acetate by 2-pyridones

Christian B. Fischer, Harald Steininger, David S. Stephenson and Hendrik Zipse*

Department of Chemistry and Biochemistry, LMU München, Butenandtstrasse 13, D-81377 Munich, Germany

Received 28 September 2004; revised 3 January 2005; accepted 16 January 2005

ABSTRACT: The influence of a series of alkyl-substituted 3-cyano-2-pyridones on the kinetics of the reaction of *p*-nitrophenyl acetate (**10**) with *n*-butylamine (**9**) was studied. The reactions were monitored under pseudo-first-order conditions using an excess of *n*-butylamine by ^{1}H NMR spectroscopy at 23 °C in $CDCl_3$. A non-linear dependence of the observed rate constants k_{obs} on the pyridone concentration was observed in all cases. The results were analysed using two different kinetic models. The first model is based on the amine-catalysed background reaction in combination with a pyridone-catalysed process, whose efficiency is reduced through dimerization of the pyridone catalyst to an inactive dimer. The second model also involves the amine-catalysed background process, now in combination with a catalysed process proceeding through pre-equilibrium complexation of the substrate with a 1:1 amine–pyridone complex and a second (rate-determining) step involving C—N bond formation. In addition to these kinetic studies, the aggregation behaviour of pyridones **2** and **3** was also studied in pure deuteriochloroform solutions and mixtures of *n*-butylamine and deuteriochloroform. While substantial aggregation to dimers occurs for both pyridones in deuteriochloroform, no such dimerization appears to occur in deuteriochloroform solutions containing 250×10^{-3} mol l^{-1} *n*-butylamine. This finding strongly supports kinetic model 2 as the more realistic choice.
Copyright © 2005 John Wiley & Sons, Ltd.
Supplementary electronic material for this paper is available in Wiley Interscience at http://www.interscience.wiley.com/jpages/0894-3230/suppmat/

KEYWORDS: catalysis; non-linear kinetics; NMR spectroscopy; aggregation behaviour; nitrogen heterocycles; pyridones; aminolysis

INTRODUCTION

Ester aminolysis is an important reaction for the synthesis of amides and peptides and has accordingly been studied for a large variety of systems.[1] Catalysis by acids and bases is frequently observed, but unattractive for the construction of sensitive and stereochemically complex structures.[2–4] The catalytic activity of pyridones was studied early on in simple model systems such as *p*-nitrophenyl acetate (**10**) and *n*-butylamine (**9**) and also more complex systems containing amino acid substrates.[5–8] It has been proposed that the catalytic efficiency of 2-pyridones is based on the property of simultaneously donating and accepting a hydrogen bond.[9] Most of the studies have concentrated on parent system **1**, which is known to equilibrate, depending on the polarity of the surrounding solvent, between the two known tautomeric forms 2-pyridone (**1a**) and 2-hydroxypyridine (**1b**) (Scheme 1).[10,11] Both of these tautomers can, of course, act as 'bifunctional' catalysts.

Tautomers **1a** and **1b** are known to aggregate readily, especially in apolar solution, the symmetric dimer **I** and the chain motive **II** being two conceivable association patterns (Scheme 1). The aggregation behaviour in solution has been studied quantitatively by UV–visible measurements in cyclohexane and decane,[10] by IR techniques in CCl_4,[12] by vapour pressure osmometry in chloroform,[13] and by ^{1}H NMR spectroscopy in THF-d_8.[9] All of these studies are in clear support of a dimeric structure in the particular solvent and hence in the liquid phase. Earlier work on the pyridone-catalysed reaction of *p*-nitrophenyl acetate (**10**) and *n*-butylamine (**9**) in chlorobenzene was limited to a narrow concentration range owing to solubility problems of the pyridone catalysts.[7] We have now synthesized a series of alkyl-substituted 2-pyridones (**2–8**) (Scheme 2), which are likely to display improved solubility in apolar media.[14] For selected candidates of this series, we first studied the aggregation behaviour in a low-polarity solvent such as $CDCl_3$, and subsequently the catalytic activity of **1–8** in the reaction of *p*-nitrophenyl acetate (**10**) with *n*-butylamine (**9**).

**Correspondence to:* H. Zipse, Department of Chemistry and Biochemistry, LMU München, Butenandtstrasse 13, D-81377 Munich, Germany.
E-mail: zipse@cup.uni-muenchen.de
Contact/grant sponsor: DFG; *Contact/grant number:* Zi 436/4-2.

Copyright © 2005 John Wiley & Sons, Ltd.

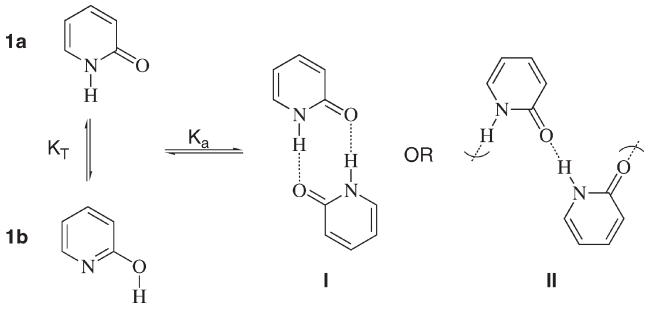

Scheme 1

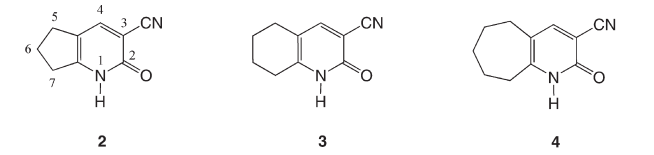

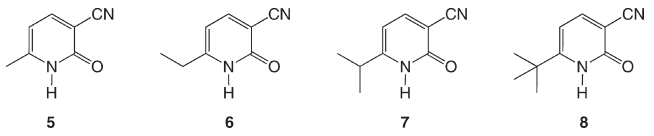

Scheme 2

RESULTS AND DISCUSSION

Association behaviour of 2-pyridones

The aggregation behaviour of pyridones **2** and **3** was studied in detail in deuteriochloroform solution. Pyridone **2** was chosen owing to its remarkably short hydrogen bonds formed in the solid state.[14] Pyridone **3** is closely related to **2** in structural terms, but shows significantly better solubility in $CDCl_3$ at 298 K (**2**, 40×10^{-3} mol l^{-1}; **3**, 120×10^{-3} mol l^{-1}). In particular when compared with simpler derivatives such as **5** (0.9×10^{-3} mol l^{-1}), the aggregation behaviour of **2** can conveniently be studied using ^{1}H NMR spectroscopy (600 MHz) in $CDCl_3$. Of particular relevance for these studies performed at 300 K and a concentration of 10×10^{-3} mol l^{-1} is the NH resonance located in the spectrum at around 13.45 ppm (typically observed as a broad signal), the resonance for the aromatic proton located at C-4 of the pyridone ring at 7.75 ppm (singlet) and the 7-CH_2 group located in close proximity to the NH unit, which can be found as a triplet at 3.02 ppm ($J = 7.5$ Hz). On lowering the temperature to −53 °C (220 K), we observe splitting of the NH signal to provide two new signals at 6.63 and 14.15 ppm. In line with previous studies of H-bonded systems, we attribute the signal at 6.63 ppm to the monomeric pyridone **2** [δ_M(**2**)] and the signal at 14.15 ppm to its dimer [δ_D(**2**)].[15] In order to characterize the equilibrium between these species in a quantitative manner, the ^{1}H NMR spectrum was measured at different concentrations (regular intervals from 1×10^{-3} to 15×10^{-3} mol l^{-1} in deuteriochloroform) at 300 K (Fig. 1).[16]

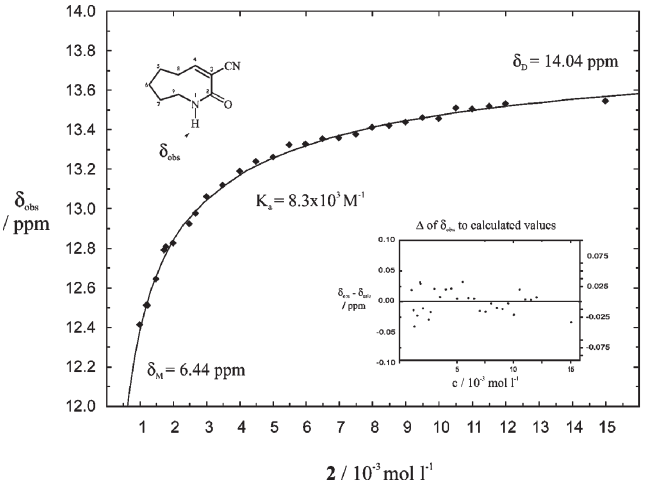

Figure 1. Concentration dependence of selected ^{1}H NMR data for **2** ($CDCl_3$, 300 K)

Following the procedure of Chen and co-workers[17] and Horman and Dreux,[18] the experimental data were fitted to a simple dimerization model described through Eqns (1) and (2) (for further details see the supplementary material, available in Wiley Interscience):

$$\delta_{obs} = \delta_D - \left(\frac{|\delta_D - \delta_M|}{2K_a}\right)^{1/2}\left(\frac{|\delta_{obs} - \delta_M|}{[M]_0}\right)^{1/2} \quad (1)$$

$$\delta_{obs} = \delta_M + f_D(\delta_D - \delta_M) \quad (2)$$

The observed shift (δ_{obs}) is expressed in terms of the monomer shift (δ_M), the dimer shift (δ_D), the total concentration of the pyridone **2**([M]$_0$), the dimerization constant (K_a) and the mole fraction of the dimer (f_D). The variable parameters in the fitting process are K_a, δ_M and δ_D (Table 1). The values of δ_M(**2**) = 6.44 ± 0.07 ppm and δ_D(**2**) = 14.04 ± 0.01 ppm obtained from these measurements are in close agreement with those obtained previously in low-temperature ^{1}H NMR studies (Table 1).

The value of the association constant K_a(**2**) = (8.3 ± 0.1) × 10^3 M^{-1} ($CDCl_3$, 300 K) is smaller than that obtained by Persico *et al.*[11c] for dipyridone systems linked by rigid spacers of $K_a = 6 \times 10^4$ M^{-1} ($CDCl_3$, 298 K), but larger than that measured for parent compound **1** of K_a(**1**) = 2.9×10^3 M^{-1} and for the closely related 3-ethoxycarbonyl-2(1*H*)-pyridone of $K_a = 1.3 \times 10^3$ M^{-1} ($CDCl_3$, 296 K).[19] The association constant

Table 1. Results for ^{1}H NMR studies of pyridones **2** and **3** performed at various temperatures (T) and concentrations [c]

Parameter	Pyridone **2**		Pyridone **3**
	Variable T	Variable [c] (T = 300 K)	Variable [c] (T = 300 K)
δ_M (ppm)	6.63	6.44 ± 0.07	6.22 ± 0.12
δ_D (ppm)	14.15	14.04 ± 0.01	13.57 ± 0.02
K_a (M^{-1})	—	8340 ± 104	7778 ± 163

Copyright © 2005 John Wiley & Sons, Ltd.

determined for **3** using the same approach is similar to that of **2** at $K_a(\mathbf{3}) = (7.8 \pm 0.2) \times 10^3\ \text{M}^{-1}$ ($CDCl_3$, 300 K). In order to support further the formation of dimers as the dominant form of aggregation in apolar solution, we follow the procedure described by Quaglia *et al.*[20] This procedure involves the correlation of the relative aggregation-induced shifts ($\Delta\delta = \delta - \delta_{min}$) of two different proton positions of **2**. A linear dependence should be observed if only dimers and no higher aggregates exist in solution. For this type of analysis, we select the signals corresponding to the amide proton and the protons at C-7. The C-7 methylene group is best suited for the analysis, because the corresponding ^{1}H NMR signal shifts significantly with changes in concentration.

The excellent linear dependence between the two ^{1}H NMR shifts with a correlation factor of 0.996 over the whole concentration range (Fig. 2) supports symmetric dimers as the main form of aggregation in apolar solvents. Following the same procedure as described already for the amide proton signal (NH), the concentration-dependent signals for the C-7 protons can be fitted to a dimerization model with the same result for $K_a(\mathbf{2}) = 8.3 \times 10^3\ \text{M}^{-1}$. The reactivity studies (see below) were performed in $CDCl_3$ containing significant concentrations of the reactants. Of these, the amine *n*-butylamine (**9**) may be the most likely to raise the overall polarity of the reaction medium. The concentration-dependent ^{1}H NMR spectra of pyridone **2** were therefore reinvestigated in the presence of $250 \times 10^{-3}\ \text{mol l}^{-1}$ of amine **9** (Fig. 3). This concentration corresponds to that used in the reactivity studies. Owing to the interference of signals belonging to the various NH groups present in solution, we must limit ourselves now to the analysis of the C-7 proton signals of **2** for concentrations above $1.5 \times 10^{-3}\ \text{mol l}^{-1}$ (Fig. 3). At this low pyridone concentration, the C-7 proton signal is located at 2.72 ppm in the presence of amine **9** (open squares in Fig. 3) and at 2.98 ppm in pure $CDCl_3$ (closed diamonds in Fig. 3). In order to facilitate the comparison of the two sets of data,

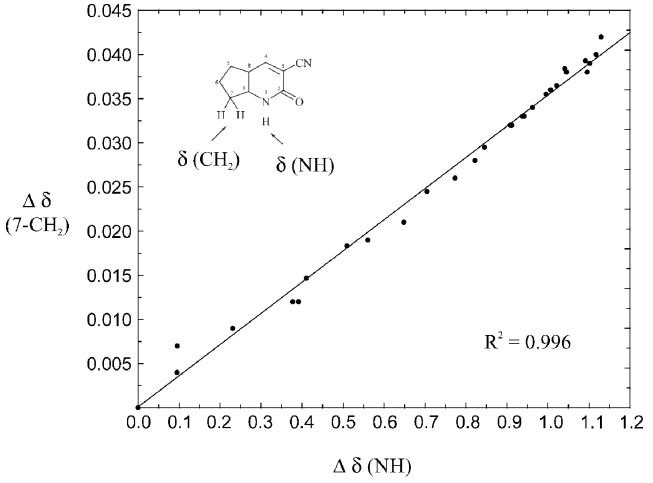

Figure 2. Correlation of the association-induced shifts of the NH proton vs the 7-CH_2 protons

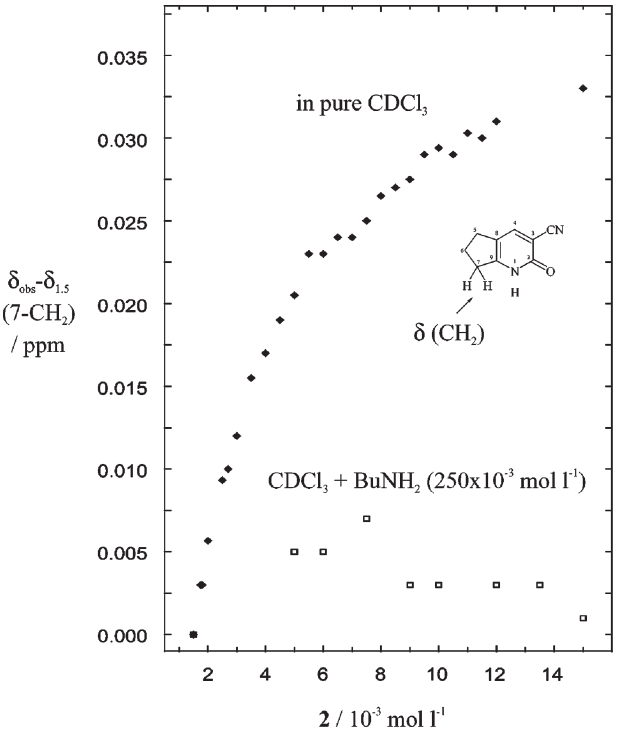

Figure 3. Concentration dependence of the 7-CH_2 ^{1}H NMR signal in the presence (open squares) and the absence (closed diamonds) of *n*-butylamine ($250 \times 10^{-3}\ \text{mol l}^{-1}$)

we use here the ^{1}H NMR shifts (δ_{obs}) relative to those measured at the lowest concentration of $1.5 \times 10^{-3}\ \text{mol l}^{-1}$ ($\delta_{1.5}$). In contrast to the situation in pure $CDCl_3$, there is hardly any concentration-induced variation of the signal for the C-7 protons in this case. This suggests that addition of $250 \times 10^{-3}\ \text{mol l}^{-1}$ of amine **9** to chloroform solutions of pyridone **2** leads to complete disruption of its hydrogen-bonded dimers. This effect can most readily be rationalized by assuming the formation of 1:1 (or higher order) complexes of **2** with amine **9**.

Reactivity studies

The catalytic activity of pyridones **1**–**8** was studied for the reaction of *n*-butylamine (**9**) with *p*-nitrophenyl acetate (**10**) in $CDCl_3$ at ambient temperature (Scheme 3).

The reaction rate was studied under pseudo-first-order conditions using amine **9** in large excess ($250 \times 10^{-3}\ \text{mol l}^{-1}$). Under these conditions, the turnover of ester **10** can be expressed as a first-order process following the simple rate law in Eqn (3):

$$[\text{ester}] = [\text{ester}]_0 \exp(-k_{obs} t) \quad (3)$$

$$k_{obs} = k_A[\text{amine}]^2 + k_{cat}[\text{amine}][\text{cat}] \quad (4)$$

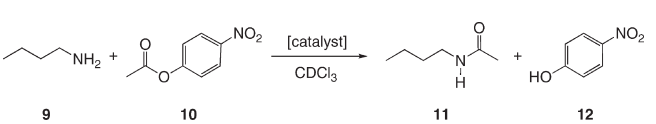

Scheme 3

Copyright © 2005 John Wiley & Sons, Ltd.

Based on earlier studies of the same reaction in chlorobenzene, we expect that the pseudo-first-order rate constant k_{obs} is composed of at least two components [Eqn (4)].[7] The first component is second order in amine and describes the self-catalysed process in the absence of any added catalyst. The second term is first order in amine and describes the (pyridone) catalysed process. Additional terms (e.g. those for the uncatalysed process being first order in amine) are not significant at the reaction conditions chosen here and are therefore neglected.[5,21] The catalytic rate constant k_{cat} reflecting the catalytic potential of pyridones **1–8** can be determined by measuring the rate constant k_{obs} as a function of the catalyst concentration. However, the results shown in Fig. 4 for pyridone **2** are clearly not in line with Eqn (4), since the rate constant k_{obs} depends on the concentration of catalyst **2** in a decidedly non-linear fashion.

This has in the past been understood as a reflection of the propensity of pyridones to form (catalytically inactive) dimers in apolar solution.[5,7] In quantitative terms, the equilibrium between monomeric pyridones (such as **1a** and **1b** in Scheme 1) and pyridone dimers (such as **I** in Scheme 1) can be described using Eqn (5). The monomer concentration [M] is given here as a function of the total pyridone concentration $[M]_0$ and the dimerization constant K_a.

$$[M] = \frac{\left(8K_a[M]_0 + 1\right)^{1/2} - 1}{4K_a} \quad (5)$$

$$\frac{k_{obs}}{[amine]} = k_A[amine] + k_{cat}\frac{\left(8K_a[M]_0 + 1\right)^{1/2} - 1}{4K_a} \quad (6)$$

Assuming that only the pyridone monomers are catalytically active, the expression for the monomer concentration [M] in Eqn (5) can be combined with Eqn (4) to yield a new expression for the dependence of the observed rate constant k_{obs} on the total pyridone concentration $[M]_0$ [Eqn (6)]. This will in the following be referred to as *kinetic model 1*. Equation (6) can be used to reproduce the change in k_{obs} with the total catalyst concentration $[M]_0$ in a non-linear fitting procedure, giving access to the rate constants k_{cat} and k_A and the dimerization constant K_a. In order to reduce the number of unknown parameters, the rate constant k_A was determined in the absence of any catalyst as $k_A = 1.066 \times 10^{-2}\,l^2\,mol^{-2}\,s^{-1}$ at 296 K. Using catalyst concentrations of up to $20 \times 10^{-3}\,mol\,l^{-1}$, the rate data for pyridones **1–8** given in Table 2 were then obtained.

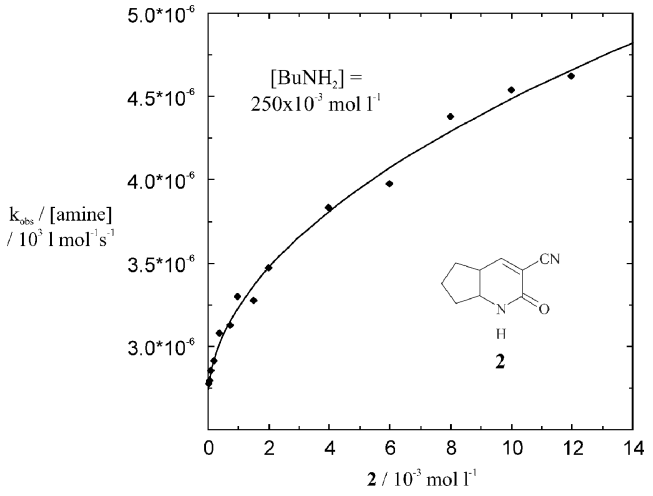

Figure 4. Dependence of the ratio k_{obs}/[amine] on the concentration of pyridone **2**. The curve corresponds to that predicted by Eqn (6)

Table 2. Rate constants k_{cat} and dimerization constants K_a for *kinetic model 1*[a]

Compound	k_{cat} ($l^2\,mol^{-2}\,s^{-1}$)	K_a ($l\,mol^{-1}$)
1	$7.8 \times 10^{-1} \pm 2 \times 10^{-2}$	230 ± 15
2	$1.3 \times 10^{1} \pm 2 \times 10^{-1}$	$244\,000 \pm 6900$
3	$1.1 \times 10^{0} \pm 2 \times 10^{-2}$	750 ± 32
4	$4.2 \times 10^{-1} \pm 1 \times 10^{-2}$	136 ± 10
5	$1.2 \times 10^{1} \pm 3 \times 10^{-1}$	$315\,000 \pm 15\,000$
6	$3.8 \times 10^{-1} \pm 2 \times 10^{-2}$	444 ± 61
7	$2.5 \times 10^{-1} \pm 9 \times 10^{-3}$	455 ± 40
8	$9.1 \times 10^{0} \pm 9 \times 10^{-1}$	$143\,000 \pm 29\,000$

[a] All results were obtained by assuming a rate constant for the background reaction of $k_A = 1.066 \times 10^{-2}\,l^2\,mol^{-2}\,s^{-1}$ (296 K, 0.25 mol l^{-1} *n*-butylamine).

The results obtained for pyridones **2** and **3** are in surprising contrast to those of the ^{1}H NMR studies. Whereas the latter predict practically no dimerization in chloroform–*n*-butylamine solutions, the K_a value obtained for **2** from *kinetic model 1* is much larger than that determined for pure chloroform solutions (244 000 vs 8340 M^{-1}). Moreover, the K_a values determined for **2** and **3** (having rather similar structures) using *kinetic model 1* are vastly different, whereas no such difference is apparent from the ^{1}H NMR results. Also, the association constants determined from *kinetic model 1* for pyridones **5–8** are difficult to explain with the structural characteristics of these compounds. It is particularly irritating to see that the association constants are much larger for the *tert*-butyl substituted pyridone **8** than for the ethyl- and isopropyl-substituted compounds **6** and **7**. Taken together, the association constants predicted from *kinetic model 1* seem unreliable, despite the fact that Eqn (6) can be used to fit the non-linear dependence of the observed rate constant k_{obs} on the total pyridone concentration in a satisfactory manner. The same must, unfortunately, also be said of the catalytic rate constants k_{cat}, whose values are determined simultaneously with K_a.

An alternative model for the non-linear dependence of the observed rate on the total catalyst concentration is based on the assumption of the pre-equilibrium complexation of the ester substrate with the pyridone catalyst (Scheme 4). At the high amine concentrations used in the

Copyright © 2005 John Wiley & Sons, Ltd.

(I) Ester + Cat* $\overset{K_C}{\rightleftharpoons}$ [Ester • Cat*] $\xrightarrow[(rds)]{k_{cat}}$ Products + Cat

(II) Ester + 2 $BuNH_2$ $\xrightarrow{k_A}$ Products

Scheme 4

experiment, the catalyst will most likely be present as a 1:1 amine–pyridone complex (The amine concentration exceeds that of the catalyst by at least 12.5-fold even at the highest catalyst concentrations used in this study).[22] This assumption is also in line with the influence of added butylamine on the NMR spectroscopic properties of pyridone **2** as described in Fig. 3. The catalyst–amine complex will in the following be designated with the 'cat*' symbol. The concentration of this species is assumed to be identical with the total pyridone concentration $[cat]_0$. Formation of the catalyst–substrate complex proceeds with equilibrium constant K_C and can be expected to be rapid as compared with the following (rate-determining) step, in which formation of the amide bond occurs. In parallel with this catalysed process (I), we must (as in *kinetic model 1*) also expect the self-catalysed aminolysis (II) to occur at substantial rates and consider the decrease of ester concentration. This completes the definition of *kinetic model 2*, which has in the past been used to rationalize the methylimidazole-catalysed hydrolysis of *p*-nitrophenyl carboxylate esters, the aminolysis of sulfamate esters in chloroform and metal ion-assisted methanolysis of acetylimidazoles.[23–25] In line with the ^{1}H NMR experiments performed in the presence of amine **9**, *kinetic model 2* does not assume any self-association of the pyridone catalysts, but quantitative formation of pyridone–amine complexes. The formation of pyridone–ester complexes is, of course, equally possible. However, given the changes observed in the ^{1}H NMR spectrum of **2** on addition of butylamine and the lack of such an effect on addition of ester **10**, we prefer the assumption of predominant pyridone–amine complex formation.

The definition of the observed rate constant k_{obs} for *kinetic model 2* is given by the equation

$$k_{obs} = \frac{k_0 + k_{cat}K_C[cat^*]}{(1 + K_C[cat^*])} \qquad (7)$$

The first variable in Eqn (7), $k_0 = k_A[amine]^2$, describes the self-catalysed process. The second term describes the pyridone-catalysed pathway with the catalytic constant k_{cat}, the complexation constant K_C and the corresponding concentration of the amine-complexed catalyst [cat*]. Owing to the nature of the latter, the amine concentration does not appear explicitly in this second term. The K_C and k_{cat} values were obtained by non-linear least-squares fitting of the experimentally determined values of k_{obs} to Eqn (7).

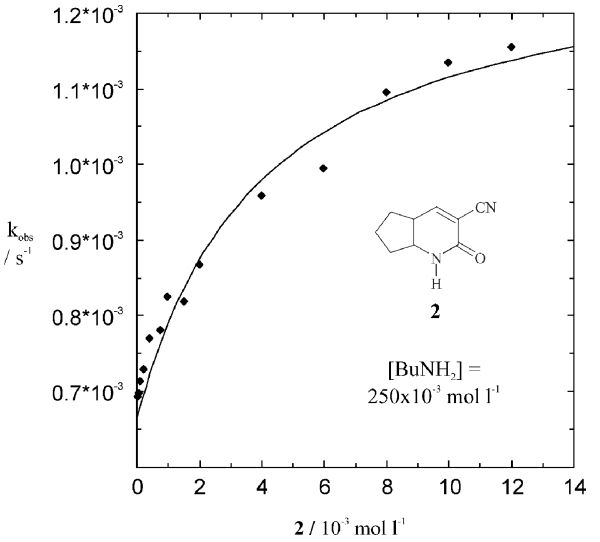

Figure 5. Dependence of the pseudo-first-order rate constant k_{obs} on the concentration of pyridone **2**. The curve corresponds to that predicted by Eqn (7)

The rate constant k_A was again held constant at its independently determined value of $k_A = 1.066 \times 10^{-2}\,l^2\,mol^{-2}\,s^{-1}$ at 296 K. The experimentally measured values for pyridone **2** and the curve predicted by Eqn (7) are shown in Fig. 5. The results obtained for pyridones **1**–**8** are given in Table 3.

The substrate–catalyst association constants K_C predicted by *kinetic model 2* are small and depend much less on the structural characteristics of catalysts **1**–**8** than the effective dimerization constant K_a (Table 2). Variations in the catalytic rate constant k_{cat} are also much smaller than predicted by *kinetic model 1* and again show little variation with the catalyst structure. The catalytic activity of pyridones **1**–**8** can best be characterized by the ratio of the rate constant for the pyridone-catalysed pathway (k_{cat}) and the effective background rate constant (k_0) as contained in Eqn (7) for the observed rate constant k_{obs}. The values reported in Table 3 were obtained for a concentration of $[\mathbf{9}] = 0.250\,mol\,l^{-1}$. In practically all cases the calculated speedup ratio k_{cat}/k_0 is modest and shows little variation with the substitution pattern of the

Table 3. Rate constants k_{cat} and complexation constants K_C for *kinetic model 2*[a]

Compound	k_{cat} (s^{-1})	K_C ($l\,mol^{-1}$)	k_{cat}/k_0[b]
1	$2.30 \times 10^{-3} \pm 3 \times 10^{-5}$	85 ± 3	3.45
2	$1.30 \times 10^{-3} \pm 2 \times 10^{-5}$	248 ± 18	1.95
3	$1.81 \times 10^{-3} \pm 2 \times 10^{-5}$	127 ± 5	2.72
4	$1.67 \times 10^{-3} \pm 2 \times 10^{-5}$	87 ± 3	2.51
5	$9.82 \times 10^{-4} \pm 1 \times 10^{-5}$	584 ± 40	1.47
6	$1.08 \times 10^{-3} \pm 2 \times 10^{-5}$	156 ± 14	1.62
7	$9.99 \times 10^{-4} \pm 1 \times 10^{-5}$	118 ± 6	1.50
8	$1.46 \times 10^{-3} \pm 7 \times 10^{-5}$	146 ± 27	2.19

[a] All results were obtained by assuming a rate constant for the background reaction of $k_A = 1.066 \times 10^{-2}\,l^2\,mol^{-2}\,s^{-1}$ (23 °C, 0.25 $mol\,l^{-1}$ *n*-butylamine).
[b] see text for definition.

Copyright © 2005 John Wiley & Sons, Ltd.

pyridone catalysts. It is particularly interesting to see that the size of the C-6 substituent does not perturb the catalytic efficiency of the catalysts. This would be more in line with a purely supramolecular mechanism of catalysis, in which the pyridone catalysts provide a hydrogen bonding environment that is more favourable for the aminolysis transition state than the substrate ground state, but cannot rule out alternative mechanisms including double hydrogen transfer (see below).[26]

CONCLUSIONS

The combination of results obtained from temperature- and concentration-dependent ^{1}H NMR measurements with those obtained from kinetic studies of the aminolysis reaction of *p*-nitrophenyl acetate in $CDCl_3$ leaves no doubt that the reactivity data for pyridones **1–8** can best be analysed using *kinetic model 2*. According to this model, the pyridone catalysts (present as 1:1 pyridone–amine complexes) form a weakly bound complex with the *p*-nitrophenyl acetate substrate. Unimolecular reaction of this substrate complex to yield the product amide **11** and *p*-nitrophenol (**12**) represents the rate-limiting step of this sequence. Comparison of the self-catalysed background reaction and the pyridone-catalysed pathway at high catalyst loadings shows that the pyridones **1–8** are not sufficiently active to accelerate the overall reaction substantially.

The low sensitivity of the catalytic rate constant k_{cat} on the substitution pattern of pyridones **1–8** can best be rationalized by assuming the stabilization of the aminolysis transition state through favourable hydrogen bonding interactions (a supramolecular effect). This is in contrast to earlier suggestions that, starting from a reactant complex such as **13** (Scheme 5), bifunctional catalysis through pyridones follows a double proton transfer mechanism through a formally eight-membered ring as depicted in structure **14**. Alternatively, the reaction may proceed through the same mechanism as in the uncatalysed case, in which amine and ester react directly through a four-membered ring transition state. As reflected in transition structure **15**, the catalytic effects of pyridones would then be the result of providing a hydrogen bonding environment particularly favourable for the aminolysis transition state. However, the experimental results obtained in this study cannot be used to rule out one of these two mechanistic options. The small variations in k_{cat} as a function of pyridone structure are, however, more easy to reconcile with transition structure **15**, in which the pyridone is not actively involved in any bond making/bond breaking processes.

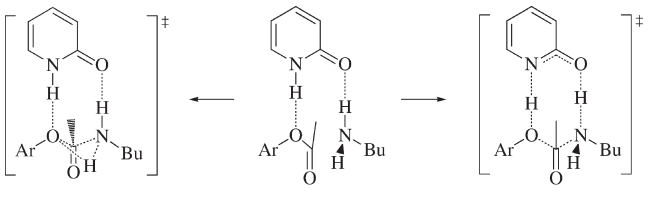

15 **13** **14**

Scheme 5

EXPERIMENTAL

Materials. Pyridones **2–8** were synthesized and purified according to the procedures described in Ref. 14. Pyridone **1** was purchased from Aldrich, recrystallized from acetone, dried *in vacuo* and stored under nitrogen prior to use.

General procedure for dimerization studies (^{1}H NMR spectroscopy). All concentration-dependent measurements for **2** and **3** were recorded on a Bruker AMX 600 (600.13 MHz) spectrometer at a constant temperature of 300.00 ± 0.05 K. Before the measurements, all solutions were freshly prepared by a dilution series from one stock solution. Deuteriochloroform was stored over CaH_2 and distilled under a nitrogen atmosphere prior to use. The same procedure was applied to prepare the samples for the low-temperature measurements on a Varian VXR 400 S spectrometer. All measurements were performed at a constant temperature of 219.75 ± 0.05 K ($-53.4\,^\circ$C) in deuteriochloroform in triplicate form.

General procedure for the kinetic studies by ^{1}H NMR spectroscopy. All kinetic measurements were recorded at a constant temperature of 296.15 K (23 °C) on a Varian Mercury 200 (199.98 MHz) spectrometer. The reaction rate was determined by following the signals for the aryl protons of *p*-nitrophenyl acetate and *p*-nitrophenol. Before the measurements, the solutions with the required concentrations of *n*-butylamine (**9**) (250×10^{-3} mol l^{-1}), *p*-nitrophenyl acetate (**10**) (50×10^{-3} mol l^{-1}) and the appropriate catalyst (various concentrations) were freshly prepared. Deuteriochloroform was stored over CaH_2 and distilled under a nitrogen atmosphere prior to use. *n*-Butylamine (**9**) was purified in the same manner. Compound **10** was recrystallized from hexane[27] and, after confirmation of the correct elemental analysis, stored under a nitrogen atmosphere prior to use. There are two basic procedures for the preparation of the solutions and the reaction mixtures, as follows.

Procedure 1. For catalysts that are sufficiently soluble in deuteriochloroform (**1–4** and **6–8**) a stock solution of known concentration can be prepared directly from the catalyst and deuteriochloroform. Variation of the catalyst concentration is achieved through dilution with $CDCl_3$. The three solutions containing the amine **9**, the ester **10** and the catalyst are mixed in equal portions of 180 µl each in the NMR tube immediately prior to use.

Copyright © 2005 John Wiley & Sons, Ltd.

Procedure 2. Catalyst **5** is less soluble in $CDCl_3$ but more soluble in *n*-butylamine–$CDCl_3$ solution. Hence preparation is achieved by dissolving an exact amount of catalyst in a well-defined volume of *n*-butylamine solution in $CDCl_3$. The amine concentration is identical with that used in the measurements. Dilution of the catalyst solution for varying concentrations is achieved in the same manner as described in Procedure 1, but now using the *n*-butylamine–deuteriochloroform solution. The reaction mixtures are prepared through addition of 25 µl of 2 M ester solution to 1 ml of the appropriate *n*-butylamine–catalyst solution in the NMR tube.

Acknowledgement

We thank the DFG for financial support of this project (Zi 436/4-2).

REFERENCES

1. (a) Bodánszky M. *Nature* 1955; **175**: 685; (b) Bodánszky M, Szelke M, Tömörkény E, Weisz E. *Chem. Ind. (London)* 1955; 1517; (c) Bodánszky M. *Chem. Ind. (London)* 1957; 524; (d) Bodánszky M, Birkhimer CA. *Chem. Ind. (London)* 1962; 1620–1621; (e) Nakamizo N. *Bull. Chem. Soc. Jpn.* 1969; **42**: 1071–1077, 1078–1082; (f) Nakamizo N. *Bull. Chem. Soc. Jpn.* 1971; **44**: 2006; (g) Siemens LM, Rottnek FW, Trzupek LS. *J. Org. Chem.* 1990; **55**: 3507–3511, and references cited therein.
2. Jencks WP. *Catalysis in Chemistry and Enzymology.* McGraw-Hill: New York, 1969.
3. Bender ML. *Chem. Rev.* 1960; **60**: 53–113.
4. (a) Bender ML, Turnquest BW. *J. Am. Chem. Soc*. 1957; **79**: 1652–1655, 1656–1662; (b) Bruice TC, Schmir GL. *J. Am. Chem. Soc*. 1957; **79**: 1663–1667.
5. Su CW, Watson JW. *J. Am. Chem. Soc*. 1974; **96**; 1854–1857.
6. Oie T, Loew GH, Burt SK, Binkley JS, MacElroy RD. *J. Am. Chem. Soc.* 1982; **104**: 6169–6174.
7. (a) Zipse H, Wang L. *Liebigs Ann.* 1996; 1501–1509; (b) Zipse H, Wang L, Houk KN. *Liebigs Ann.* 1996; 1511–1522.
8. (a) Gandour RD, Walker DA, Nayak A, Newkome GR. *J. Am. Chem. Soc.* 1978; **100**: 3608–3609; (b) Hogan JC, Gandour RD. *J. Org. Chem.* 1991; **56**: 2821–2826; (c) Hogan JC, Gandour RD. *J. Org. Chem.* 1992; **57**: 55–61.
9. Ducharme Y, Wuest JD. *J. Org. Chem.* 1988; **53**: 5787–5789.
10. Beak P. *Acc. Chem. Res.* 1977; **10**: 186–192.
11. (a) Gallant M, Viet MTP, Wuest JD. *J. Am. Chem. Soc.* 1991; **113**: 721–723; (b) Simard M, Su D, Wuest JD. *J. Am. Chem. Soc.* 1991; **113**: 4696–4698; (c) Persico F, Wuest JD. *J. Org. Chem.* 1993; **58**: 95–99; (d) Brunet P, Simard M, Wuest JD. *J. Am. Chem. Soc.* 1997; **119**: 2737–2738.
12. Kulevsky N, Reineken W. *J. Phys. Chem.* 1968; **72**: 3339–3340.
13. Beak P, Covington JB, Smith SG, White JM, Zeigler JM. *J. Org. Chem.* 1980; **45**: 1354–1362.
14. Fischer CB, Polborn K, Steininger H, Zipse H. *Z. Naturforsch., Teil B* 2004; **59**: 1121–1131.
15. (a) Tkadlecová M, Dohnal V, Costas M. *Phys. Chem. Chem. Phys.* 1999; **1**: 1479–1486; (b) Fielding L. *Tetrahedron* 2000; **56**: 6151–6170.
16. Conners KA. *Binding Constants*. Wiley: New York, 1987.
17. (a) Chen JS, Shirts RB. *J. Phys. Chem*. 1985; **89**: 1643–1646; (b) Chen JS, Rosenberger F. *Tetrahedron Lett.* 1990; **31**: 3975–3978.
18. Horman I, Dreux B. *Helv. Chim. Acta* 1984; **67**: 754–764.
19. Loppinet-Serani A, Charbonnier F, Rolando C, Huc I. *J. Chem. Soc., Perkin Trans 2* 1998; 937–942.
20. Quaglia M, Chenon K, Hall AJ, De Lorenzi E, Sellergren B. *J. Am. Chem. Soc*. 2001; **123**: 2146–2154.
21. Menger FM, Smith JH. *J. Am. Chem. Soc.* 1972; **94**: 3824–3829.
22. Biechler SS, Taft RW Jr. *J. Am. Chem. Soc*. 1957; **79**: 4927–4935.
23. Gagliano RA, Knowlton RC, Byers LD. *J. Org. Chem.* 1989; **54**: 5247–5250.
24. Spillane WJ, Hogan G, McGrath P, King J. *J. Chem. Soc., Perkin Trans 2* 1998; 309–313.
25. Khan A, Neverov AA, Yatsimirsky AK, Brown RS. *Can. J. Chem.* 1999; **77**: 1005–1008.
26. (a) Engdahl KA, Bivehed H, Ahlberg P, Saunders WH Jr. *J. Am. Chem. Soc*. 1983; **105**: 4767–4774; (b) Kuzuya M, Noguchi A, Okuda T. *Bull. Chem. Soc. Jpn.* 1984; **57**: 3461–3465.
27. Chen ET, Pardue HL. *Anal. Chem.* 1994; **66**: 3318–3322.

Copyright © 2005 John Wiley & Sons, Ltd.